Mathematical Biosciences and Engineering

Mathematical Biosciences and Engineering, 16(4): 2927–2941.
DOI: 10.3934/mbe.2019144
Received: 28 December 2018
Accepted: 25 February 2019
Published: 10 April 2019

http://www.aimspress.com/journal/MBE

Research article

Effect of nano-particles on MHD flow of tangent hyperbolic fluid in a ciliated tube: an application to fallopian tube

K. Maqbool[1,*], S. Shaheen[1], A. M. Siddiqui[2]

[1] Department of Mathematics & Statistics, International Islamic University, Islamabad 44000, Pakistan
[2] Department of Mathematics, York Campus, Pennsylvania State University, York, Pennsylvania 17403, U. S. A

***Correspondence:** Email: khadija.maqbool@iiu.edu.pk.

Abstract: This study shows the effects of magnetic field and copper nanoparticles on the flow of tangent hyperbolic fluid (blood) through a ciliated tube (fallopian tube). The present study will be very helpful for those patients who are facing blood clotting in fallopian tube that may cause for infertility or cancer. The nanoparticles and magnetic field are very helpful to break the clots in blood flowing in fallopian tube. Since blood flows in fallopian tube due to ciliary movement, therefore medicines containing copper nanoparticles and magnetic field with radiation therapy help to improve the patient. Ciliary movement has a particular pattern of motion i.e., metachronal wavy motion which helps to fluid flow. For the forced convective MHD flow of tangent hyperbolic nano-fluid, momentum and energy equations are solved by the small Reynolds' number approximation and Adomian decomposition method by constructing the recursive relation of ADM and solved by software "MATHEMATICA". The effects of parameters such as nanoparticle volume fraction, Hartmann number, entropy generation and Bejan's number have been discussed through graphs plotted in software "MATHEMATICA". It is found that blood flow is accelerated and heat transfer enhancement is maximum in the presence of nano particles, also magnetic effects accelerates the blood flow and help to enhance the heat transfer whereas the presence of porous medium increases the fluid's velocity and reduce the transfer of heat through fluid flow.

Keywords: nano particles; MHD; tangent hyperbolic fluid; ciliated axisymmetric tube; porous medium

1. Introduction

Heat transfer enhancement in biological fluids is an important area of modern biomechanics and biomedical engineering. The study of thermodynamics deals with properties of the substances associated with pressure, density, velocity, viscosity and temperature and their relationship with energy which can be studied from the literature [1,2]. Heat regulation is essential to all mammals and furthermore heat transfer has found many applications in modern biomedical engineering. For example heat flow in blood, heat transfer during eye treatment, respiratory thermal control and thermal bio convection [3–5]. Since some conventional fluids like water and blood have low thermal conductivities which decreases the enhancing performance. During last decade the field of nanoparticle was improved remarkably and a new kind of solid-liquid mixture is formed which is called nano fluid. By adding nanoparticles in the base fluids the thermal conductivity of base fluid will alter remarkably.

Nano-fluids are colloidal suspensions of nano-sized solid particles in a liquid, which was first studied by Choi [6]. More recently conducted experiments [7] have indicated that nano-fluids tend to have higher thermal conductivity than the base fluids. Among the many advantages of nano-fluids over conventional solid-liquid suspensions, the following are worth mentioning, higher specific surface area, higher stability of the colloidal suspension, reduced particle clogging compared to conventional colloids, and higher level of control of the thermodynamics and transport properties by varying the particle material, concentration, size and shape. Maiga et al. [8] studied the heat transfer enhancement in turbulent flow through tube using Al_2O_3 nanoparticle suspension. There are lot of nanoparticles in blood that are commonly one thousand times smaller than a human hair and the presence of nanoparticles produce many severe diseases such as neutropenia, blood cancer, eosinophilia, leukocytes etc. In many cases common method cannot be used to eliminate these particles. Presently nanotechnology is being used to separate these nanoparticles from plasma [9].

Ciliary movement has been a subject of special interest in the society of experimental biology. Cilia presumably first discovered by famous Dutch microscopist Antoni van Leeuwenhoek in 1675. Cilia occurs in row, fields or tracks at the surface of living cells, where their usual function of propelling the fluid over the cell surface is achieved by unilateral lashing action. Cilia exhibits different beating patterns depending on the surrounding geometry as described in literature [10–12]. The cycle of beat of single cilium separated into effective and recovery stroke. During the effective phase the cilium is erect, maximizing its height, moving relatively quickly and bending to its base. Before a cilium can perform a second effective stroke the cilium must first progress through a recovery stroke. In the recovery phase the cilium maintains a low profile, moves more slowly and propagates a bend from base to tip drawing the cilium backwards in an unrolling action.

Different metachronal patterns can be recognized in protozoa and classified according to angle of power stroke in relation to the direction of metachronal transmission. In literature antiplectic wave pattern is widely used as compared to the symplectic metachrony because the prior is classified by the separation of collective cilia during the forward stroke, permitting them to push more fluid capacity and thus mounting the stroke effectiveness [13,14].

A thin layer of mucous is present at the inner surface of fallopian tube and ciliated cells of different lengths are present around the mucous membrane. In the fallopian tube ciliary motion helps to transport spermatozoa towards ampulla and also cilia induced flow transports ovum from ovaries at the time of ovulation. At ampulla, if fertilization occurs, then ciliary motion helps to transfer the

embryo to the last region of fallopian tube i.e. intermural [15–17]. The ovary and uterus veins anastomose to form a network of blood vessels around the ovarian artery to facilitate the concentration of substances and communication within the female reproductive tract. Maqbool et al. [18–20] investigated the effect of ciliary motion on non-Newtonian fluid models.

Entropy generation in nano-fluid flow which is flowing through wavy channels are studied by many researchers [21,22]. Later on, many researchers [23,24] analyzed the heat transfer enhancement in MHD nano-fluids flowing in porous ducts or tubes. They found that entropy generation enhances due to the nanoparticles. A large number of attempts have been made to study the effect of nanoparticles with MHD but very less attention is paid to study the effect of nanoparticles in bio fluid.

It is evident that microorganisms when causes infection in human body, can die with the application of constant magnetic field strength. It is observed by the medical doctors that tuberculosis skin lesion is completely recovered by the antibiotic having constant negative strength of magnetic field. It is also observed by the physicians that for throat infection when pulmonary cilia are not working properly antibiotics containing magnetic field help to die out the virus that effects the pulmonary cilia movement. Recently, several researchers [25–27] introduced the study of ciliary movement where they used the magnetic field to observe the ciliary frequency. Later on, many researchers studied the effects of entropy generation of MHD flows in the presence of nanoparticles and porous medium [28–40].

The activity of cilia and ciliated cells normally occurred in conditions where viscous forces greatly predominate over inertial forces i.e. Reynolds' number is less than one because of small size and low speed. Thus, the purpose of this work is to analyse the characteristics of MHD fluid flow of tangent hyperbolic nano-fluid with enhanced heat transfer due to ciliary motion in a porous medium. While the analysis could be applied to copper-blood nano-fluid due to the accessibility of its physical properties.

2. Mathematical model

Consider a tangent hyperbolic nano-fluid flow in a tube of mean radius a in a porous medium. Assume infinite number of continuously beating cilia are present at the inner walls of tube generating symplectic metachronal wave which moves towards positive z-axis with wave speed c. Uniform magnetic field of strength B_0 is applied in transverse direction i.e. along the perpendicular direction of fluid motion.

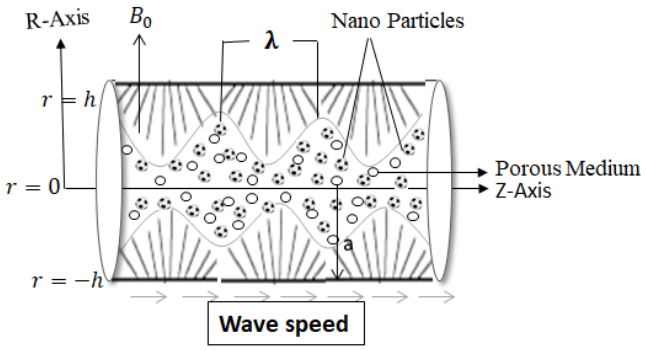

Figure 1. Geometry of ciliated tube.

In existing literature many researchers [18,19] studied the motion of tips of cilia which are tracing the path of ellipse.

Governing equations for an incompressible MHD tangent hyperbolic nano-fluid through porous medium are defined as [41]

$$\nabla.\boldsymbol{V} = 0, \tag{1}$$

where

$$V = [u, 0, w], \tag{2}$$

and

$$\rho_f \frac{d\boldsymbol{V}}{dt} = div\boldsymbol{S} + \sigma(\boldsymbol{J} \times \boldsymbol{B}) + R, \tag{3}$$

$$(\rho c)_f \frac{dT}{dt} = k_{nf}\nabla^2 T + trace(\boldsymbol{\tau}.\boldsymbol{L}) \tag{4}$$

where **V** is the velocity components, w is the axial component of velocity, u is the radial component of velocity, $\boldsymbol{S}$ is the Cauchy stress tensor, $\frac{d}{dt} = \frac{\partial}{\partial t} + V.\nabla$ is the total derivative, ρ_f is the density of nano-fluid, σ is the electrical conductivity of fluid, $\boldsymbol{J}$ is the current density, $\boldsymbol{B}$ is the strength of magnetic field, R is the Darcy's resistance, T is the temperature profile and L is gradient of velocity.

Here the appropriate stress tensors for the tangent hyperbolic model are defined as [34,35]

$$\boldsymbol{S} = -p\boldsymbol{I} + \boldsymbol{\tau}, \tag{5}$$

$$\boldsymbol{\tau} = [(\eta_\infty + (\eta_0 + \eta_\infty)\tanh(\Gamma\dot{\gamma})^m)], \tag{6}$$

in which $\boldsymbol{\tau}$ is the extra stress tensor, η_0 represents zero shear rate viscosity, η_∞ is the infinite shear rate viscosity, Γ is time constant and m shows the power law index.

$$\dot{\gamma} = \sqrt{\frac{1}{2}\boldsymbol{\pi}}, \quad where\ \boldsymbol{\pi} = trace(grad\boldsymbol{V} + grad\boldsymbol{V}^T)^2, \tag{7}$$

where $\boldsymbol{\pi}$ is second order tensor we study the above equation for the case where $\eta_\infty = 0$ and $\Gamma\dot{\gamma} < 1$. The elements of extra stress tensor can be written as

$$\dot{\gamma}_i = \boldsymbol{L} + \boldsymbol{L}^T \tag{8}$$

$$\bar{\tau} = \eta_0((\Gamma\dot{\gamma})^m)\dot{\gamma}_i = \eta_0(1 + \Gamma\dot{\gamma} - 1)^m\dot{\gamma}_i = \eta_0\big(1 + m(\Gamma\dot{\gamma} - 1)\big)\dot{\gamma}_i \tag{9}$$

where thermal conductivity of Cu+blood nano-fluid is defined as follows

$$\rho_{nf} = (1 - \phi)\rho_f + \phi\rho_s, \quad \eta_{nf} = \frac{\eta_f}{(1 - \phi)^{2.5}},$$

$$\left(\rho c_p\right)_{nf} = (1-\phi)\left(\rho c_p\right)_f + \phi\left(\rho c_p\right)_s, \qquad \alpha_{nf} = \frac{k_{nf}}{\left(\rho c_p\right)_{nf}} \tag{10}$$

$$k_{nf} = k_f\left(\frac{k_s + 2k_f - 2\phi\left(k_f - k_s\right)}{k_s + 2k_f + 2\phi\left(k_f - k_s\right)}\right)$$

where k_{nf} is the thermal conductivity of nano-fluid, k_f is the thermal conductivity of base fluid, k_s is the thermal conductivity of solid nano particles and ϕ is the solid volume fraction.

The Mathematical model for geometry of cilia tips in the wave frame is

$$h = 1 + \varepsilon \cos 2\pi z \tag{11}$$

$$w(h) = -1 - 2\pi\varepsilon\alpha\beta \cos 2\pi z$$

where ε is the cilia length parameter, α is the eccentricity of elliptic wave and β is the wave number.

The governing equations of motion of tangent hyperbolic fluid model in a tube are specified as follows.

$$\frac{\partial u}{\partial r} + \frac{u}{r} + \frac{\partial w}{\partial z} = 0, \tag{12}$$

$$\rho_f\left[u\frac{\partial w}{\partial r} + w\frac{\partial w}{\partial z}\right] = -\frac{\partial p}{\partial z} + \frac{1}{r}\frac{\partial}{\partial z}(r\tau_{rz}) + \frac{\partial \tau_{zz}}{\partial z} - \left(\sigma {B_0}^2 + \frac{\eta_f}{k}\right)(w + c), \tag{13}$$

$$\rho_f\left[u\frac{\partial u}{\partial r} + w\frac{\partial u}{\partial z}\right] = -\frac{\partial p}{\partial r} + \frac{1}{r}\frac{\partial}{\partial r}(r\tau_{rr}) + \frac{\partial \tau_{zr}}{\partial z}, \tag{14}$$

$$(\rho c)_f\left[u\frac{\partial T}{\partial r} + w\frac{\partial T}{\partial z}\right] = k_{nf}\left(\frac{1}{r}\frac{\partial}{\partial r}\left(r\frac{\partial T}{\partial r}\right) + \frac{\partial^2 T}{\partial z^2}\right) + \tau_{zr}\frac{\partial w}{\partial r}. \tag{15}$$

where ρ_f is the fluid density, u and w are the radial and axial components of velocity, c is the wave speed, η_f is the apparent viscosity of fluid and k is the permeability parameter.

The following non-dimensional parameters can be introduced for further analysis.

$$z^* = \frac{z}{\lambda},\ r^* = \frac{r}{a},\ u^* = \frac{u}{\beta c},\ w^* = \frac{w}{c},\ h^* = \frac{h}{a},\ p^* = \frac{a\beta}{c\mu}p,$$
$$\beta = \frac{a}{\lambda},\ S_{ij}{}^* = \frac{a}{\mu c}S_{ij},\ \lambda_1 = \frac{c\lambda_1}{a},\ Re = \frac{\rho a\beta}{\mu},\ We = \frac{\Gamma c}{a},\ \alpha_f = \frac{k}{(\rho c)_f},$$
$$\theta = \frac{T - T_0}{T_0},\ M = \sqrt{\frac{\sigma}{\mu}}aB_0{}^2,\ D_a = \frac{k}{a^2},\ Br = \frac{a^2\eta_f}{k_f T_0},\ Pr = \frac{\mu c_p}{k_f},$$
$$Ec = \frac{c^2}{c_p T_0}. \tag{16}$$

where λ, a, c symbolize the wavelength, width of velocity and wave speed respectively, Re is the Reynolds' numbers, β is the wave number while D_a is the Darcy's number. In terms of dimensionless parameters the momentum equations and shear stresses are

$$\frac{\partial u}{\partial r} + \frac{u}{r} + \frac{\partial w}{\partial z} = 0, \tag{17}$$

$$Re\beta\left[u\frac{\partial w}{\partial r} + w\frac{\partial w}{\partial z}\right] = -\frac{\partial p}{\partial z} + \frac{1}{r}\frac{\partial}{\partial z}(r\tau_{rz}) + \beta\frac{\partial \tau_{zz}}{\partial z} - \left(M^2 + \frac{1}{D_a}\right)(w+1), \tag{18}$$

$$Re\beta^2\left[u\frac{\partial u}{\partial r} + w\frac{\partial u}{\partial z}\right] = -\frac{\partial p}{\partial r} + \frac{\beta}{r}\frac{\partial}{\partial r}(r\tau_{rr}) + \beta^2\frac{\partial \tau_{zr}}{\partial z} - \beta\frac{\partial \tau_{\theta\theta}}{\partial z}, \tag{19}$$

$$\beta(\rho c)_f\left[u\frac{\partial \theta}{\partial r} + w\frac{\partial \theta}{\partial z}\right] = k_{nf}\left(\frac{1}{r}\frac{\partial}{\partial r}\left(r\frac{\partial \theta}{\partial r}\right) + \beta^2\frac{\partial^2\theta}{\partial z^2}\right) + \tau_{zr}\frac{\partial w}{\partial r}, \tag{20}$$

$$\tau_{rz} = \left(1 + m\left(We\frac{\partial w}{\partial r} - 1\right)\right)\frac{\partial w}{\partial r}, \tag{21}$$

Using long wavelength approximation (β→0) the governing equations and boundary conditions are as follows

$$\frac{\partial p}{\partial z} = (1-m)\frac{1}{r}\frac{\partial}{\partial r}\left(r\frac{\partial w}{\partial r}\right) + mWe\frac{1}{r}\frac{\partial}{\partial r}\left(r\left(\frac{\partial w}{\partial r}\right)^2\right) - \left(M^2 + \frac{1}{D_a}\right)(w+1), \tag{22}$$

$$-\frac{\partial p}{\partial r} = 0, \tag{23}$$

$$\frac{k_{nf}}{k_f}\frac{1}{r}\frac{\partial}{\partial r}\left(r\frac{\partial \theta}{\partial r}\right) = -Br\frac{\eta_{nf}}{\eta_f}\left(1 + m\left(We\frac{\partial w}{\partial r} - 1\right)\right)\left(\frac{\partial w}{\partial r}\right)^2, \tag{24}$$

$$\frac{\partial w}{\partial r} = 0, \quad \frac{\partial \theta}{\partial r} = 0 \quad at \ r = 0,$$

$$w = w(h), \qquad \theta = 0 \quad at \ r = h. \tag{25}$$

Integration of Eq. (17) over the tube width is given as:

$$\int_0^h \left[\frac{1}{r}\frac{\partial (ru)}{\partial r} + \frac{\partial w}{\partial z}\right] r dr = 0, \tag{26}$$

$$hu(h) + \frac{1}{2}\frac{\partial q}{\partial z} - h\frac{\partial h}{\partial z}w(h) = 0, \tag{27}$$

where $q = 2\int_0^h rwdr$. Eq. (27) can be written as

$$\frac{\partial q}{\partial z} = 2h\left(\frac{\partial h}{\partial z}w(h) - u(h)\right) \tag{28}$$

The relation between q and dimensionless volume flow rate Q is given by

$$Q = 2\int_0^h RWdR = 2\int_0^h (w+1)rdr = q + h^2, \tag{29}$$

The mean volume flow rate for the time period $T = \frac{\lambda}{c}$ is

$$\bar{Q} = \frac{1}{T}\int_0^T Q dt^* = q + 1 + \frac{\varepsilon^2}{2}, \tag{30}$$

where λ is the wavelength of metachronal wave, c is the wave speed and t^* is the mean averaged time.

3. Solution of the problem

To obtain the solution of governing equations we use Adomian decomposition method [42].

$$\mathcal{L}_{rw} - \frac{\partial p}{\partial z} + mWe\frac{1}{r}\frac{\partial}{\partial r}\left(r\left(\frac{\partial w}{\partial r}\right)^2\right) - \left(M^2 + \frac{1}{D_a}\right)(w+1) = 0. \tag{31}$$

The Linear and inverse operator are chosen as follows

$$\mathcal{L}_{rw} = \frac{1}{r}\frac{\partial}{\partial r}\left(r(1-m)\frac{\partial w}{\partial r}\right), \tag{32}$$

$$\mathcal{L}_{rw}^{-1} = \int \left[\frac{1}{r(1-m)}\int r[.]\,dr\right]dr. \tag{33}$$

Applying $\mathcal{L}_r^{-1}$ on Eq. (31) we get

$$w = c_1 \ln r + c_2 - \mathcal{L}_{rw}^{-1}\left[\frac{M^2}{1-m}w + \frac{m}{1-m}mWe\frac{1}{r}\frac{\partial}{\partial r}\left(r\left(\frac{\partial w}{\partial r}\right)^2\right) + \frac{m}{1-m}\mathcal{L}^{-1}{}_{rw}\left(M^2 + \frac{1}{D_a}\right)\right]. \tag{34}$$

Adomian decomposition method yields the following infinite series

$$w = \sum_{n=0}^{\infty} w_n \tag{35}$$

Initial guess and recursive relation can be chosen in a following manner.

$$w_0 = c_1 \ln r + c_2 \frac{1}{1-m}\left(M^2 + \frac{1}{D_a}\right)\frac{r^2}{4} \tag{36}$$

$$w_{n+1} = -\mathcal{L}_r^{-1}\left[\frac{M^2}{1-m}w_n + \frac{m}{1-m}We\frac{1}{r}\frac{\partial}{\partial r}\left(r\left(\frac{\partial w_n}{\partial r}\right)^2\right)\right]. \tag{37}$$

With the help of boundary conditions and initial guess solution takes the following form.

$$w_0 = \frac{1}{4(1-m)}\frac{dp}{dz}(r^2 - h^2) + w(h) \tag{38}$$

$$w = w(h) + A_1(r^2 - h^2) + A_2(r^3 - h^3) + A_3(r^4 - h^4) + A_4(r^5 - h^5) + A_5(r^6 - h^6) + \cdots \tag{39}$$

Using Eq. (39) in Eq. (24) we get

$$\begin{aligned}\theta = {} & A_6(r^4 - h^4) + A_7(r^5 - h^5) + A_8(r^6 - h^6) + A_9(r^7 - h^7) + A_{10}(r^8 - h^8) \\ & + A_{11}(r^9 - h^9) + A_{12}(r^{10} - h^{10}) + A_{13}(r^{11} - h^{11}) \\ & + A_{14}(r^{12} - h^{12}) + A_{15}(r^{13} - h^{13}) + A_{16}(r^{14} - h^{14}) \\ & + A_{17}(r^{15} - h^{15}) + A_{18}(r^{16} - h^{16}) + A_{19}(r^{17} - h^{17}) + \cdots.\end{aligned} \tag{40}$$

Integrating Eq. (39) using software "**MATHEMATICA**" calculating pressure gradient as

$$\frac{dp}{dz} = -\frac{C_2}{3C_1} - \frac{2^{\frac{1}{2}}\left(-{C_2}^2 + 3C_1C_3\right)}{3C_1\left(C_5 + \sqrt{4(C_6)^3 - (C_7)^2}\right)^{\frac{1}{3}}} + \frac{\left(C_8 + \left(C_5 + \sqrt{4(C_9)^3 - (C_{10})^2}\right)^{\frac{1}{3}}\right)}{3 \times 2^{\frac{1}{3}}C_1} \tag{41}$$

4. Entropy generation

Entropy Generation can be written as

$$S'''_{gen} = \frac{k_f}{T_\infty^2}\left(\left(\frac{\partial T}{\partial r}\right)^2 + \left(\frac{\partial T}{\partial r}\right)^2\right) + \frac{1}{T_0}\tau_{zr}\frac{\partial w}{\partial r}. \tag{42}$$

Dimensionless form of Entropy Generation can be written as

$$N_S = \frac{S'''_{gen}}{S'''_G} = \left(\frac{\partial \theta}{\partial r}\right)^2 + Br\Lambda\left(1 + m\left(We\frac{\partial w}{\partial r} - 1\right)\right)\left(\frac{\partial w}{\partial r}\right)^2 \tag{43}$$

$$S'''_G = \frac{k_f T_0^2}{\bar{\theta}_0^2 a^2}, \qquad \Lambda = \frac{\bar{\theta}_0}{T_0} \tag{44}$$

5. Graphical results

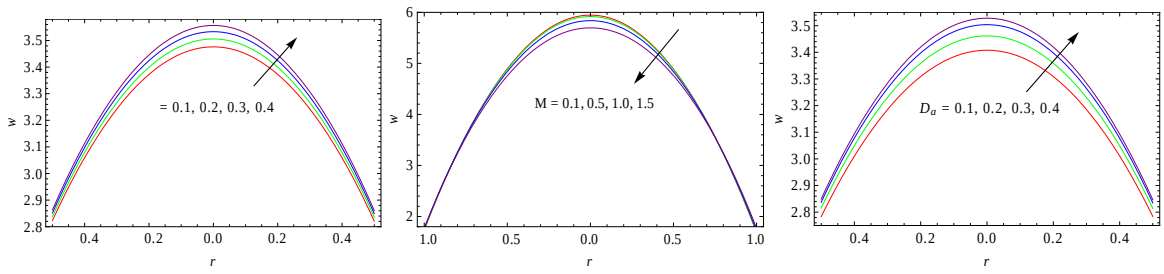

(a) **(b)** **(c)**

Figure 2. Variation of axial velocity w with r.

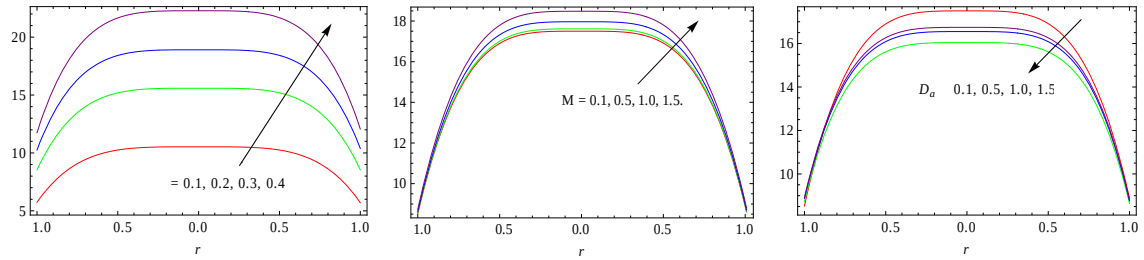

(a) **(b)** **(c)**

Figure 3. Variation of temperature θ with r.

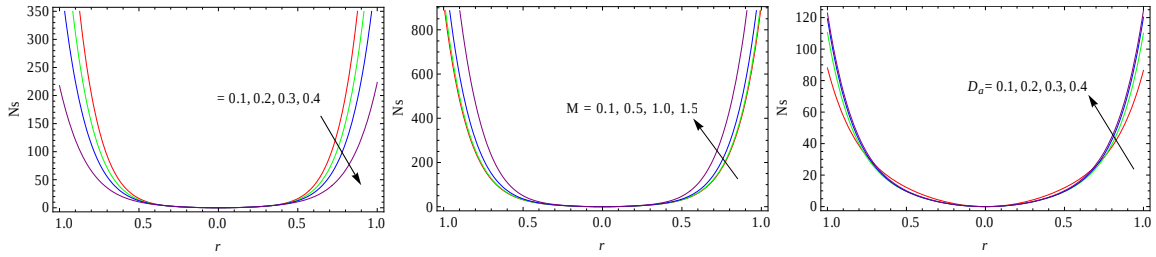

(a) **(b)** **(c)**

Figure 4. Variation of Entropy generation Ns with r.

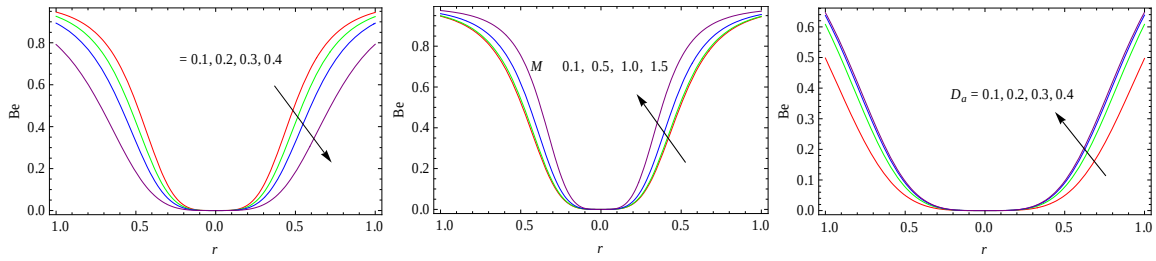

(a) **(b)** **(c)**

Figure 5. Variation of Bejan number Be with r.

5. Discussion

In this section the graphical results have shown the effects of different parameters of interest. The cilia induced flow of a tangent hyperbolic nano-fluid in circular tube is investigated. The effect of emerging parameters for the entropy generation, temperature and velocity profile are observed.

Axial velocity for various values of, nanoparticle volume fraction of the fluid ϕ, Hartmann number M and Darcy's number D_a are observed in figure (2a)−(2c). Figure (2a) shows that velocity increases by increasing nanoparticle volume fraction of the fluid because when nanoparticles are high in fluid, they will move quickly that increases the velocity of the fluid. Figure (2b) shows that velocity of fluid decreases by increasing Hartmann number M because Lorentz force always opposes the fluid motion and figure (2c) shows that velocity increases by increasing Darcy's number, velocity of fluid increases because as Darcy's number increases which means more porous is the medium and fluid permeability increases and fluid through porous layer meets little resistance.

Temperature profile for different values of nanoparticle volume fraction of the fluid φ, Hartmann number M, and Darcy's number D_a are observed in figure (3a)−(3c). It can be seen that temperature is maximum at the centre of tube and minimum at the ciliated walls where it is effected by ciliated walls. Figure (3a) illustrates that by increasing nanoparticle volume fraction of the fluid φ temperature profile decreases. It can be seen in graphs that by inserting nanoparticles in blood heat

transfer increases due to which wall temperature falls. Figure (3b) shows that by increasing Hartmann number M temperature profile increases as some supplementary work has to be done by the fluid to drag it against Lorentz force which in result increases kinetic energy which is dissipated as heat. Figure (3c) shows that by increasing Darcy's number temperature profile decreases. This is due to decrease in thermal boundary layer thickness.

In Figure (4a)−(4c) entropy generation for different values of, nanoparticle volume fraction of the fluid φ, Hartmann number M, and Darcy's number D_a are observed. It can be depicted that entropy generation is maximum at the ciliated walls and minimum at the centre of tube. It is noted in figure (4a) entropy generation increases by increasing nano-fluid volume fraction. As ϕ increases effective thermal conductivity of blood rises due to which rate of heat transfer increases and temperature decreases therefore entropy generation decreases. In figure (4b) it can be seen by increasing Magnetic parameter entropy generation rises. Due to increase in Hartmann number temperature of fluid rises thus entropy generation is increased. In figure (4c) it is noticed that entropy generation increases by increasing Darcy's number. As by increasing Darcy's number thermal boundary layer thickness reduces therefore heat transfer increases and temperature decreases which rises entropy generation.

In Figure (5a)−(5c) Bejan number for different values of nanoparticle volume fraction of the fluid φ, Hartmann number M, and Darcy's number D_a are observed. Since Bejan number is defined as the ratio of heat transfer irreversibility to the net irreversibility (i.e. heat transfer irreversibility and fluid friction irreversibility). As heat transfer across a finite temperature difference is small and frictional forces are also negligible at centre due to which Bejan number decreases at the middle of the tube and at the walls of tube Bejan number is maximum. It is noted in figure (5a) that Bejan number decreases with an increase in nanoparticles volume fraction ϕ which shows that total entropy generation in blood flow is greater than entropy generation with the help of heat transfer. From figures (5b) and (5c) it can be noted that by increasing Hartmann number M and Darcy's number D_a Bejan number increases which shows that entropy generation due to heat transfer is greater than net entropy generation.

6. Conclusions

In this study we have developed a mathematical model of forced convective flow of tangent hyperbolic fluid through a ciliated axisymmetric tube in a porous medium. Effects of copper nano particles, MHD and porous media are observed for the blood flow (tangent hyperbolic fluid) in a fallopian tube. The fluid motion is produced by the ciliated surface which is considered as a continuous envelope formed by the coordinated cilia. The boundary conditions are considered at the centre of the tube and on the tip of cilia which is anchored in the wall of the tube and formed a wavy surface. The simulation shows that energy and momentum equations involves physical parameter like velocity, temperature, pressure, thermal conductivity to see the effects of nano particles, MHD and porous medium for the enhancement of heat transfer. The present study can be validated by the work of [43] if $M\rightarrow 0$ i.e. Tanh parameter is zero. Following observations are highlighted in the present study.

I. The large distribution of nanoparticles into the base fluid (blood) enhance the heat transfer.

II. The blood flow along the tube has been accelerated by increasing the volume fraction of nanoparticles.

III. The speed of the fluid flow has been decelerated by imposing the applied magnetic field in the transverse direction of the flow whereas heat transfer has increased by applying the magnetic field.

IV. The blood flow requires less amount of pressure due to the presence of nano particles.

V. The presence of nanoparticles in base fluid results in weak disorder which helps to reduce viscous dissipation effects.

The present study is very helpful to observe the blood flow in fallopian tube for those patients who are facing blood clotting in fallopian tube that may cause for infertility or cancer. Theoretical analysis of present study have shown that the nano particles and field of moving charged particles (magnetic field) help to break the clots in blood. Since flow of blood in fallopian tube is due to ciliary movement, therefore medicines containing copper nanoparticles and magnetic field with radiation therapy help to improve the patient by reducing the viscosity of blood.

Acknowledgements

We are very grateful to the editor and reviewers for their valuable and constructive comments to improve the quality of our paper.

Conflict of interest

All authors declare no conflicts of interest in this paper.

References

1. S. M. Mousazadeh, M. M. Shahmardan, T. Tavang, et al., Numerical investigation on convective heat transfer over two heated wall-mounted cubes in tandem and staggered arrangement, *Theor. Appl.*, **8** (2018), 171–183.
2. S. S. Ghadikolaei, S. S. Hosseinzadeh, K. Ganji, et al., Fe_3O_4-$(CH_2OH)_2$ nano-fluid analysis in a porous medium under MHD radiative boundary layer and dusty fluid, *J. Mol. Liq.,* **258** (2018), 172–185.
3. A. Karampatzakis and T. Samaras, Numerical model of heat transfer in the human eye with consideration of fluid dynamics of the aqueous humour, *Phys. Med. Bio.,* **55** (2010), 5653.
4. Tripathi, S. K. Pandey and O. A. Bég, Mathematical modelling of heat transfer effects on swallowing dynamics of viscoelastic food bolus through the human oesophagus, *Int. J. Therm. Sci.*, **70** (2013), 41–53.
5. A. Zaman, N. Ali, O.A. Bég, et al., Heat and mass transfer to blood flowing through a tapered overlapping stenosed artery, *Int. J. Heat. Mass. Tran.*, **95** (2016), 1084–1095.
6. S. U. S. Choi and J. A. Estman, Enhancing thermal conductivity of fluids with nanoparticles, *ASME-Publications-Fed,* **231** (1995), 99–106.

7. W. Dongsheng and Y. Ding, Experimental investigation into convective heat transfer of nano-fluids at the entrance region under laminar flow conditions, *Int. J. Heat. Mass. Tran.*, **47** (2004), 5181–5188.
8. S. Ma ̈ga, T. Nguyen, N. Galanis, et al., Heat transfer enhancement in turbulent tube flow using Al_2O_3 nanoparticle suspension, *Int. J. Numer. Method. H.*, **16** (2006), 275–292.
9. S. Ibsen, A. Sonnenberg, C. Schutt, et al., Recovery of drug delivery nanoparticles from human plasma using an electrokinetic platform technology, *Small*, **11** (2015), 5088–5096.
10. M. A. Sleigh, J. R. Blake and N. Liron, The propulsion of mucus by cilia, Amer. *Rev. Resp. Dis.*, **137** (1988), 726–741.
11. C. Brennen and H. Winet, Fluid mechanics of propulsion by cilia and flagella, *Annu. Rev. Fluid. Mech.*, **9** (1977), 339–398.
12. M. J. Sanderson and M. A. Sleigh, Ciliary activity of cultured rabbit tracheal epithelium: beat pattern and metachrony, *J. Cell. Sci*., 47 (1981), 331–347.
13. A. Murakami and K. Takahashi, Correlation of electrical and mechanical responses in nervous control of cilia, *Nature*, **257** (1975), 48.
14. J. Blake, A model for the micro-structure in ciliated organisms, *J. Fluid. Mech.*, **55** (1972), 1–23.
15. R. A. Lyons, E. Saridogan and O. Djahanbakhch, The reproductive significance of human Fallopian tube cilia, *Hum. Reprod. Update*, **12** (2006), 363–372.
16. M. B. Carlson, Human Embryology and Developmental Biology, *Elsevier Health Sciences*, 2012.
17. R. A. Lyons, E. Saridogan and O. Djahanbakhch, The effect of ovarian follicular fluid and peritoneal fluid on Fallopian tube ciliary beat frequency, *Hum. Reprod.*, **21** (2005), 52–56.
18. K. Maqbool, S. Shaheen and A. B. Mann, Exact solution of cilia induced flow of a Jeffrey fluid in an inclined tube, *Springerplus*, **5** (2016), 1379.
19. K. Maqbool, A. B. Mann and A. M. Siddiqui, et al., Fractional generalized Burgers' fluid flow due to metachronal waves of cilia in an inclined tube, *Adv. Mech. Eng.*, **9** (2017), 1687814017715565.
20. A. M. Siddiqui, A. Sohail and K. Maqbool, Analysis of a channel and tube flow induced by cilia, *Appl. Math. Comp.*, **309** (2017), 133–141.
21. A. A. Khan, F. Zaib and A. Zaman, Effects of entropy generation on Powell Eyring fluid in a porous channel, *J. Braz. Soc. Mech. Sci. Eng.*, **39** (2017), 5027–5036.
22. M. S. Alam, M. A. Alim and M. A. Hakim, Entropy generation analysis for variable thermal conductivity MHD radiative nano-fluid flow through channel, *J. Appl. Fluid. Mech.*, **9** (2016).
23. N. S. Akbar, Z. H. Khan and S. Nadeem, Influence of magnetic field and slip on Jeffrey fluid in a ciliated symmetric channel with metachronal wave pattern, *J. Appl. Fluid. Mech.*, **9** (2016), 565–572.
24. N. S. Akbar, M. Shoaib and D. Tripathi, et al., Analytical approach to entropy generation and heat transfer in CNT-nano-fluid dynamics through a ciliated porous medium, *J. Hydrodyn.*, **30** (2018), 296–306.
25. U. Mercke, The influence of varying air humidity on mucociliary activity, *Acta. Oto-Laryngol.*, **79** (1975), 133–139.

26. S. N. Khaderi, C. B. Craus, J. Hussong, et al., Magnetically-actuated artificial cilia for microfluidic propulsion, *Lab. Chip.*, **11** (2011), 2002–2010.
27. N. S. Akbar, D. Tripathi, Z. H. Khan, et al., Mathematical model for ciliary-induced transport in MHD flow of Cu-H_2O nano-fluids with magnetic induction, *Chinese. J. Phys.*, **55** (2017), 947–962.
28. M. Hassan, A. Zeeshan, A. Majeed, et al., Particle shape effects on ferrofuids flow and heat transfer under influence of low oscillating magnetic field, *J. Magn. Mater.*, **443** (2017), 36–44.
29. S. Rashidi, S. Akbar, M. Bovand, et al,. Volume of fluid model to simulate the nano-fluid flow and entropy generation in a single slope solar still, *Renew. Energ.*, **115** (2018): 400–410.
30. M. Hassan, M. Marin, R. Ellahi, et al., Exploration of convective heat transfer and flow characteristics synthesis by Cu--Ag/water hybrid-nano-fluids, *Heat. Transf. Res.*, **49** (2018).
31. A. Majeed, A. Zeeshan, A. Z. Sultan, et al., Heat transfer analysis in ferromagnetic viscoelastic fluid flow over a stretching sheet with suction, *Neural. Comput. Appl.*, **30** (2018): 1947–1955.
32. A. Zeeshan, N. Ijaz, T. Abbas, et al., The sustainable characteristic of bio-bi-phase flow of peristaltic transport of MHD Jeffrey fluid in the human body, *Sustainability-Basel.*, **10** (2018), 2671.
33. M. Akbarzadeh, S. Rashidi, N. Karimi, et al., Convection of heat and thermodynamic irreversibilities in two-phase, turbulent nano-fluid flows in solar heaters by corrugated absorber plates, *Adv. Powder. Technol.*, **29** (2018), 2243–2254.
34. S. Z, Alamri, R. Ellahi, N. Shehzad, et al., Convective radiative plane Poiseuille flow of nano-fluid through porous medium with slip: An application of Stefan blowing, *J. Mol. Liq.*, **273** (2019), 292–304.
35. N. Shehzad, A. Zeeshan, R. Ellahi, et al., Modelling study on internal energy loss due to entropy generation for non-darcy poiseuille flow of silver-water nano-fluid: An application of purification, *Entropy*, **20** (2018), 851.
36. M. M. Bhatti, A. Zeeshan, R. Ellahi, et al., Mathematical modeling of heat and mass transfer effects on MHD peristaltic propulsion of two-phase flow through a Darcy-Brinkman-Forchheimer porous medium, *Adv. Powder. Technol.*, **29** (2018), 1189–1197.
37. R. Ellahi, S. Z. Alamri, A. Basit, et al., Effects of MHD and slip on heat transfer boundary layer flow over a moving plate based on specific entropy generation, *J. Taibah. Uni. Sci.*, (2018), 1–7.
38. C. Fetecau, R. Ellahi, M. Khan, et al., Combined porous and magnetic effects on some fundamental motions of Newtonian fluids over an infinite plate, *J. Porous. Media.*, **21** (2018).
39. S. Z. Alamri, A. A. Khan, M. Azeez, et al., Effects of mass transfer on MHD second grade fluid towards stretching cylinder: A novel perspective of Cattaneo--Christov heat flux model, *Phys. Lett. A.*, **383** (2019), 276–281.
40. S. Z. Alamri, R. Ellahi, N. Shehzad, et al., Convective radiative plane Poiseuille flow of nano-fluid through porous medium with slip: An application of Stefan blowing, *J. Mol. Liq.*, **273** (2019), 292–304.

41. T. Hayat, M. Shafique, A. Tanveer, et al., Magnetohydrodynamic effects on peristaltic flow of hyperbolic tangent nano-fluid with slip conditions and Joule heating in an inclined channel, *Int. J. Heat. Mass. Tran.*, **102** (2016), 54–63.
42. A. M. Wazwaz, Partial Differential Equations and Solitary Waves Theory, *Beijing and Springer, Verlag Berlin Heidelberg*, 2009.
43. A. M. Siddiqui, A. A. Farooq and M. A. Rana, Study of MHD effects on the cilia-induced flow of a Newtonian fluid through a cylindrical tube, *Magnetohydrodynamics*, **50** (2014), 249–261.

AIMS Press